Feasibility of Ultra Long-Span Suspension Bridges Made of All Plastics

Ken-ichi MAEDA
Professor Dr. Eng.
Tokyo Metropolitan Univ.
Tokyo, Japan

Torahiko IKEDA
Bridge Engineer M. Eng.
Chodai Co., Ltd.
Ibaraki, Japan

Hitoshi NAKAMURA
Research Associate M. Eng.
Tokyo Metropolitan Univ.
Tokyo, Japan

Seishi MEIARASHI
Team Leader Ph. D.
Public Works Research Institute
Ibaraki, Japan

Summary

In this study, we examined the feasibility of ultra long-span suspension bridges made using fiber-reinforced plastic. After we confirmed the necessity of making in plastics all, a 3-span 2-hinged suspension bridge with the center span of 5,000m and the sag ratio of 1/20 was trially designed, and the static structural characteristics were elucidated. Moreover, by applying coupled flutter analysis, various countermeasures for ensuring high aerodynamic stability were investigated, and the feasibility was discussed considering all results.

Keywords: ultra long-span bridge; suspension bridge; tubular stiffening girder; fiber-reinforced plastic; CFRP; GFRP; structural characteristics; aerodynamic stability

1. Introduction

The progress of the development of fiber-reinforced plastics (FRPs) has been considerable in recent years, and they are spotlighted as new materials for civil engineering structures [1]. In particular, by using carbon-fiber-reinforced plastic (CFRP) cables in the main cable of a suspension bridge instead of steel cables, it has been indicated that dead loads can be drastically reduced, as the center span becomes longer and longer, because of the ultralight weight of such cables. [2].

Furthermore, for bridges with the span of 5,000m, it is easily confirmed [3] that CFRP must also be used in the stiffening girder as well as the main cable, even if new types (for example, the Dischinger type [4]) are applied, when the sag ratio becomes lower due to constraint of the tower height. However, such lightening may lower the aerodynamic stability, which would greatly influence the feasibility, and it is also expected that adequate countermeasures for ensuring higher stability will become necessary.

From the above-mentioned viewpoint, we examined the feasibility of ultra long-span suspension bridges made using fiber-reinforced plastics all. First, after we confirmed the necessity of making in plastics all, a 3-span 2-hinged suspension bridge with the center span of 5,000m was trially designed as follows. CFRP cables were used in the main cable with the sag ratio of 1/20, and CFRP and concrete composite columns were adopted for the tower. In the stiffening girder, vehicles were assumed to run the inside through a tubular beam [5] made of CFRP. CFRP was also used in the deck slab, but in the floor system, glass-fiber-reinforced plastic (GFRP) was used.

Next, on the basis of this trial design, analytical modeling was conducted by varying sectional values and boundary conditions of the stiffening girder, and the static structural characteristics were examined under various design loads. Moreover, the aerodynamic stability was investigated by applying the coupled flutter analysis [6], and the effects of various countermeasures on the improvement of stability were verified in order to sufficiently ensure it. Finally, from all results, the feasibility of all-plastic suspension bridges of the 5,000m-span class was discussed, including problems remaining for the future.

2. Necessity of Making in All Plastics

To ensure higher feasibility of suspension bridges of the 5,000m-span class, the tower height must be restrained to about 300m by decreasing the sag ratio to about 1/20. Currently, the predominant ratio is 1/10 and the tower height far exceeds 500m, making the feasibility low.

For the center span of a suspension bridge, by assuming the shape of the main cable to be a parabola, the maximum tension T and its relationship with the allowable stress σ_a are obtained as

$$T = \frac{(w_c + w_s)\lambda^2}{8f}\sqrt{1+16\left(\frac{f}{\lambda}\right)^2} = \frac{(w_c + w_s)\lambda}{8n}\sqrt{1+16n^2} \quad (1),$$

$$T/A \le \sigma_a \quad (2),$$

where λ, n (=f / λ), A, w_c and w_s are the span length, the sag ratio, the sectional area, the own weight of the main cable and the sum total of dead and live loads of the stiffening girder, respectively.

Eq. (2) becomes the following equation because w_c=$\gamma_c A$, when the unit weight of the main cable is set as γ_c :

$$\lambda \le \frac{8n\sigma_a A}{(w_c + w_s)\sqrt{1+16n^2}} = \frac{8n\sigma_a}{\gamma_c(1+w_s/w_c)\sqrt{1+16n^2}} \quad (3).$$

Therefore, considering n and w_s/w_c to be parameters, curves of the critical span length λ_{cr} are plotted in Fig.1 and Fig.2, where values of γ_c and σ_a are taken from Table 1 for steel cables and CFRP cables.

From these figures, it is easily confirmed that CFRP must also be used in the stiffening girder as well as in the main cable, in order to restrain the tower height to about 300m for bridges with span of 5,000m. This is because, with the sag ratio of 1/20, the self-support becomes all, when steel

Table 1 Unit Weight and Allowable Stress

		Steel	CFRP
γ_c;	Unit Weight [N/m^3]	77	15.7
σ_t;	Tensile Strength [N/mm^2]	2156	2450
ν;	Safety Factor	2.2	2.5
σ_a;	Allowable Stress [N/mm^2]	980	980

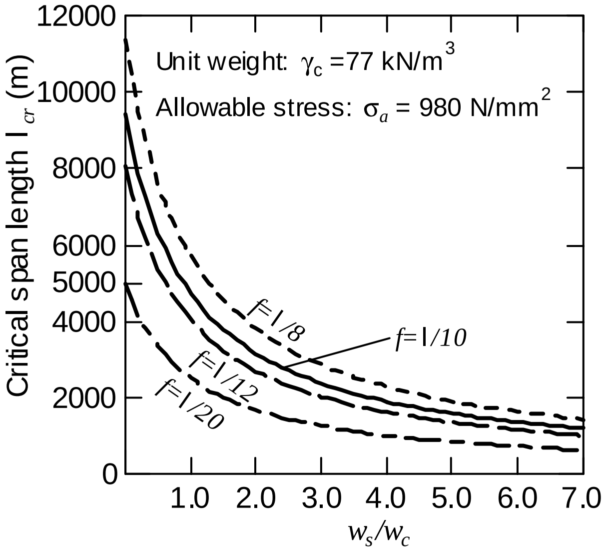

Fig.1 Critical Span Length (Steel cables)

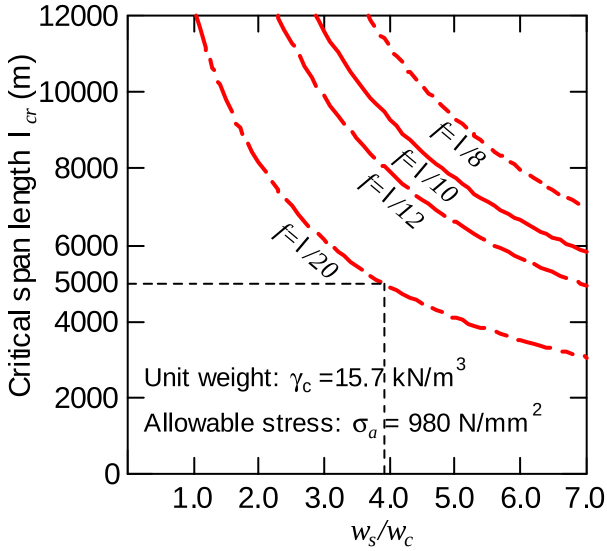

Fig.2 Critical Span Length (CFRP cables)

cables are used, and further reduction of dead loads is required, even when CFRP cables are used.

3. Trial Design and Material Property

In this study, a 3-span 2-hinged suspension bridge with the center span of 5,000m and the sag ratio of 1/20, shown in Fig.3, was trially designed and as an object of the examination.

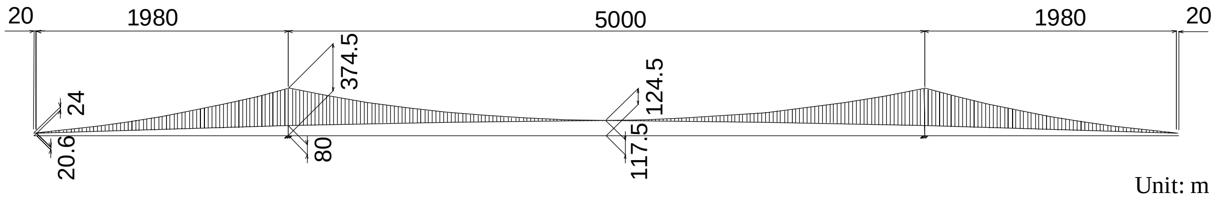

Fig.3 Trial Design

CFRP cables were used in the main cable, and CFRP and concrete composite columns were adopted for the tower. The tower was designed as steel-reinforced concrete columns, but the amount of steel reinforcement was replaced with the CFRP plate thickness. As shown in Fig.4, a tubular beam made of CFRP was used as the stiffening girder in order to decrease design wind loads, and to ensure torsional rigidity. Four lanes of traffic were assumed to pass through the tube. CFRP was also used in the deck slab. In contrast, in the floor system, which is not a structural member, GFRP was used because of its low cost.

Table 2 shows the properties of structural materials used in the main cable, the stiffening girder and the tower. CFRPs used in the stiffening girder and the tower were the same, and their cross sections were assumed to be composed of connecting pulltruded profiles. However, two values of the safety factor ν, 6.0 and 7.5, of the CFRP used in the stiffening girder were adopted, because the appropriate value has not yet been clearly determined.

By carrying out a rough design under the various design loads listed Table 3, the sectional area of the main cable was found to be about 0.8m^2. The cross section of the stiffening girder, shown in Fig.5, was decided based on the stress due to the bending moment under design wind loads, and so as to increase the plate thickness in a narrow range, when the value of the safety factor ν was 7.5. Fig.6 shows the cross section of the tower.

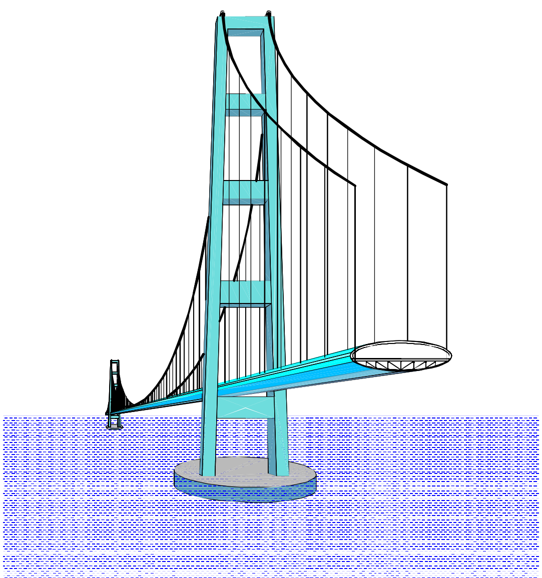

Fig.4 Schematic View

Table 2 Material Properties

	Main Cable	Stiffening Girder		Tower
Kind of Material	CFRP	CFRP		CFRP/ Concrete
Unit Weight [N/m^3]	15.7	15.7		15.7/ 23.0
Elastic Coefficient [GPa]	160	64		64/ 30
Elastic Shear Coefficient [GPa]	-	29		29/ 13
Thermal Expansion Coefficient [1/Deg.]	0.1x10^6	0.1x10^6		-
Tensile (Compressive) Strength [N/mm^2]	2450	1020		1020/ 60
Safety Factor; ν	2.2	6.0	7.5	6.0/ 3.3
Allowable Stress [N/mm^2]	980	170	136	170/ 18

Consequently, there is no problem from the viewpoint of construction, including the structures of bands and saddles in which each strand is stored separately, because the sectional area of the main cable is sufficiently smaller than 1.0m^2. Also, excess of allowable stress can be easily coped by making the stiffening girder locally nonuniform when the safety factor is required to be higher.

Table 3 Design Loads

		Main Cable		Stiffening Girder	
		Center Span	Side Span	Center Span	Side Span
Dead Load (Uniform Section)		26.74	27.18	80.47	80.50
Live Load	Concentrated Load [kN/m/Br.]	-	-	127.54	
	Distributed Load [kN/m/Br.]	-	-	20.00	
Wind Load	Design Basic Wind Speed: U_{10} [m/sec]	46			
	Standard Height: Z [m]	236.63		98.75	
	Drag Force Coefficient: C_D	0.7		1.0	
	Wind Load [kN/m/Br.]	4.09		48.83	
	Incremental Coefficient of Allowable Stress	-		1.5	

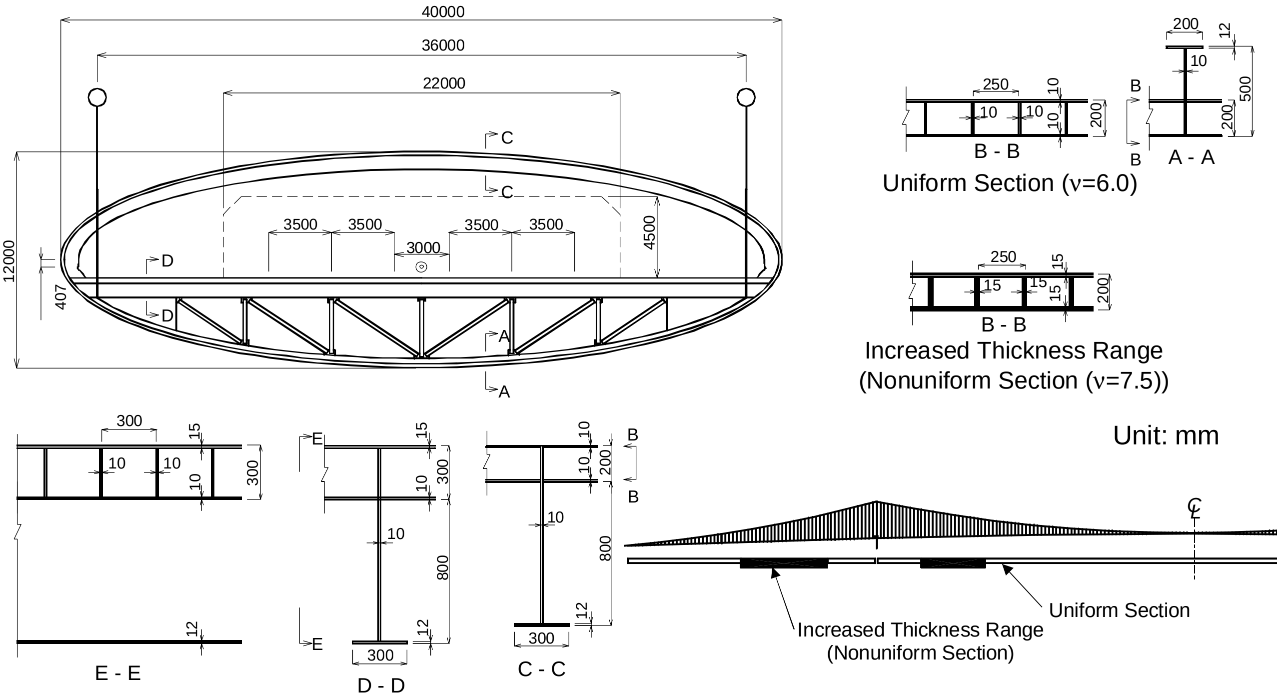

Fig.5 Cross Section of Stiffening Girder

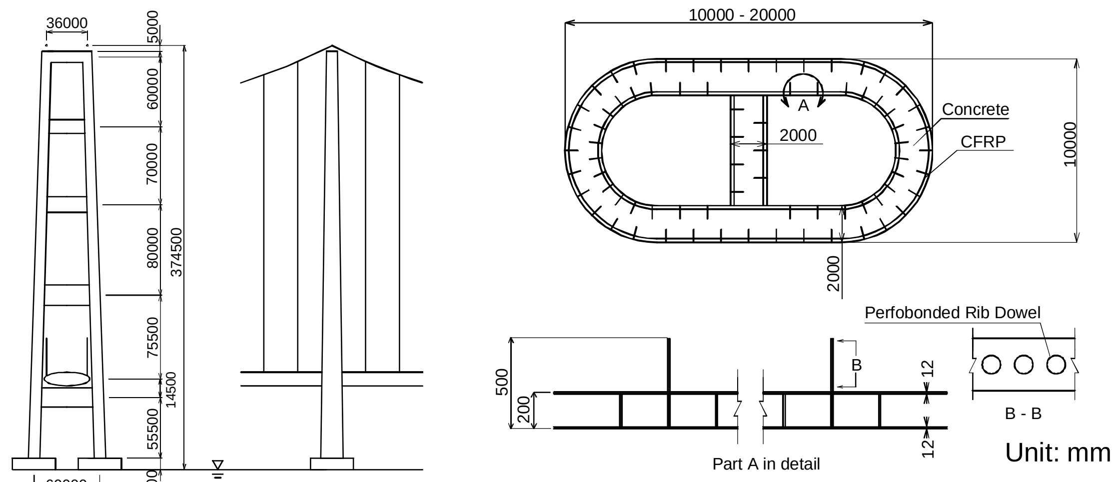

Fig.6 Cross Section of Tower

4. Static Structural Characteristics

To examine the static structural characteristics, a finite displacement analysis was carried out using 3-D frame models, as shown in Fig.7, in which the stiffening girder was regarded as a fish-bone model. Table 4 shows the sectional values of each member derived from the result of trial design. As shown in this table, two cases of the cross section of the stiffening girder were made uniform and nonuniform sections. Furthermore, the case in which the stiffening girder was assumed to be continuous was also examined for reference.

The analytical results are shown in Fig.8 to Fig.13. As the primary feature from these figures, it is

Table 4 Sectional Values

	Stiffening Girder		Main Cable	Hanger	Tower
	Uniform	Nonunif.			
E (GPa)	64	64	160	160	30
A (m^2)	3.70	3.70, 4.91	0.794	0.006	65.64 - 99.14
I_{in} (m^4)	53.70	53.70, 80.73	-	-	517.3 - 1053.
I_{out} (m^4)	530.89	530.89, 714.35	-	-	869.5 - 6469.
G (GPa)	29	29	-	-	13
J (m^4)	176.50	176.50, 265.86	-	-	1180. - 3027.

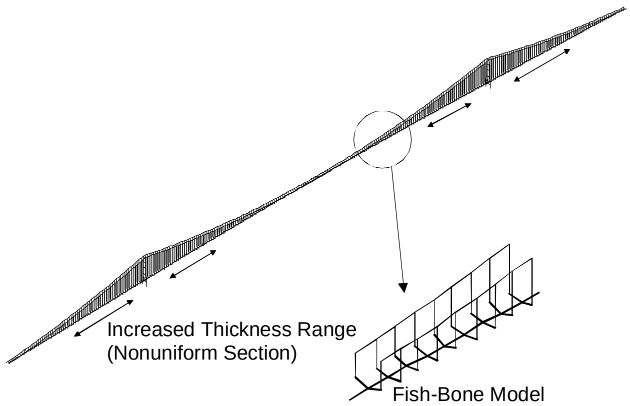

Fig.7 Analytical Model

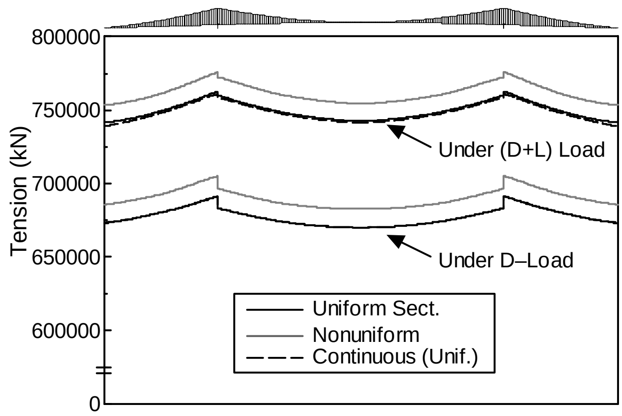

Fig.8 Tension of Main Cable under Dead & Live Loads

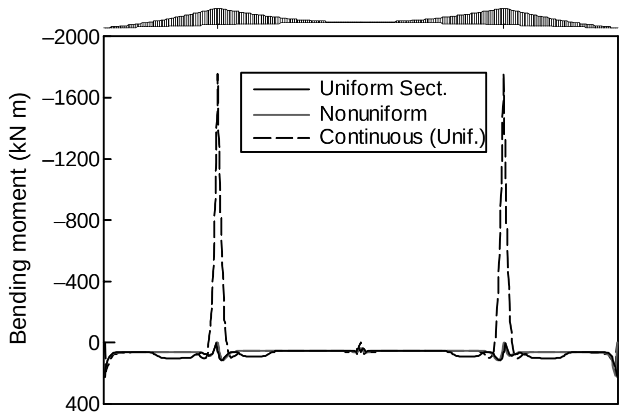

Fig.9 Bending Moment of Stiffening Girder under Thermal Change of +30Deg.

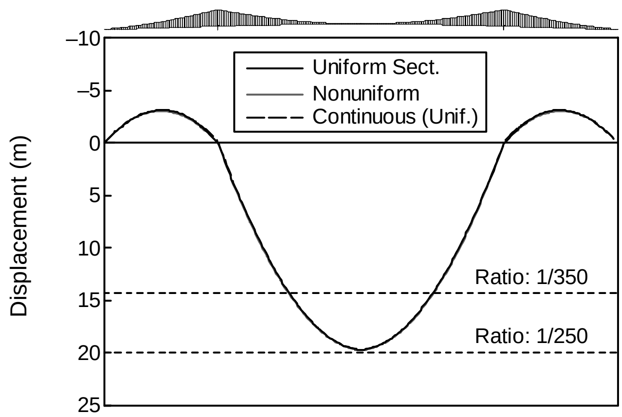

Fig.10 Deflection of Stiffening Girder under Live Loads

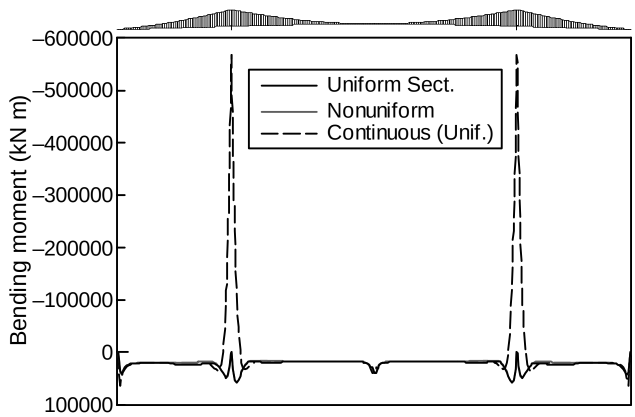

Fig.11 Bending Moment of Stiffening Girder under Live Loads

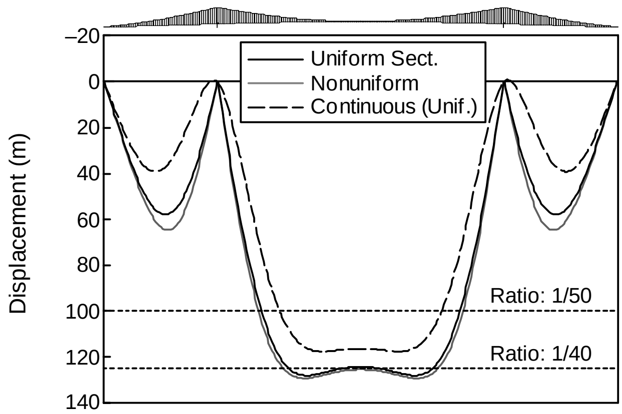

Fig.12 Deflection of Stiffening Girder under Wind Loads

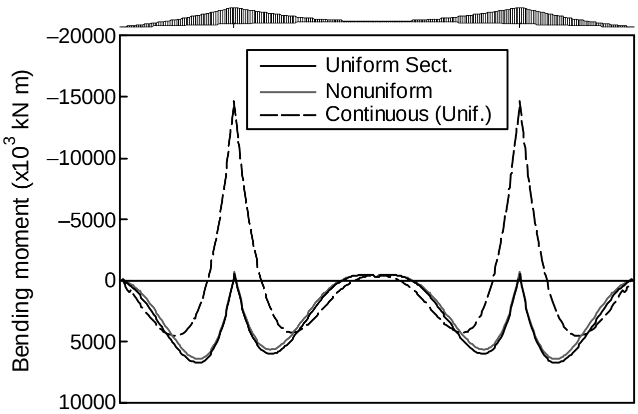

Fig.13 Bending Moment of Stiffening Girder under Wind Loads

found that displacements due to deflection are large both in-plane and out of plane, but they are not quantities which become the problems due to the vehicle travel and structural reliability. Moreover, it is also proved that the effect in which their displacements are reduced is negligible; only the negative bending moment at the intermediate support rapidly increases even if the stiffening girder is designed to be continuous.

5. Aerodynamic Stability against Coupled Flutter

To investigate the aerodynamic stability, the coupled flutter analysis of the three models described below was carried out on the basis of the modal analysis, by applying the unsteady force based on the plate-wing theory, and by considering the natural vibration mode up to the 40th mode.

The three models are based on a uniform section described in Chapter 4 (the basic model) and two models in which the structural countermeasures shown in Fig.14 and Fig.15 were adopted (the ST-1 model and the ST-2 model). Namely, in the ST-1 model, the cross hangers were concentrated at 2 optimum positions, and in the ST-2 model, the cross hangers and the horizontal cross-stays were positioned throughout length of the bridge.

Table 5 and Fig.16 respectively show the critical wind velocity *Ucr*, the natural frequency of the basic modes and the U-δ curves of the three models with structural damping of logarithmic decrement 0.02. The table and figure indicate that the aerodynamic stability against coupled flutter decreases markedly, but by adopting the structural countermeasures, the critical wind velocity can be ensured to the value of about 60m/sec.

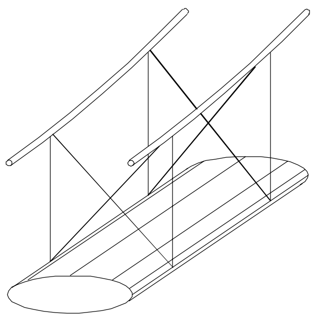

Fig.14 Cross Hanger

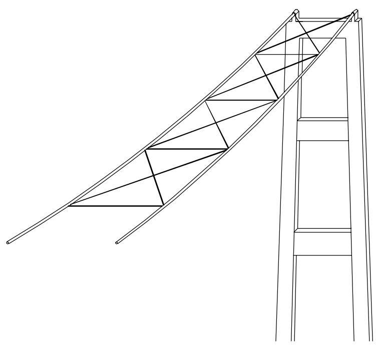

Fig.15 Horizontal Cross-Stay

Table 5 Analytical Results

		Basic Model	ST-1 Model	ST-2 Model
Critical Wind Velocity: *Ucr* [m/sec]		37.7	53.3	59.1
Natural Frequency	1st Symm. Deflection Mode [Hz]	0.0511	0.0512	0.0512
	1st Symm. Torsion Mode [Hz]	0.1784	0.1822	0.1954

Fig.17 shows the critical wind velocity *Ucr* of the three models where only the torsional rigidity was changed. It indicates that the aerodynamic stability is not sufficiently improved, by increasing only the torsional rigidity of the stiffening girder due to the variation of the shape of the cross section or the elastic shear coefficient of CFRP.

Fig.18 shows the critical wind velocity *Ucr* of the three models in the case of redesign by changing the plate thickness of the stiffening girder, and Fig.19 shows the *U*-δ curve of the ST-2 model in the case where only structural damping was changed.

These figures indicate that if the plate thickness of the stiffening girder is about 2 or 3 times the value decided from the static design, the critical wind velocity can be ensured to the value of about 70m/sec or 80m/sec. In contrast, it is also proved that the critical wind velocity can be ensured to about 70m/sec without greatly reducing the economical efficiency when structural damping is sufficiently increased by installing an adequate damper system.

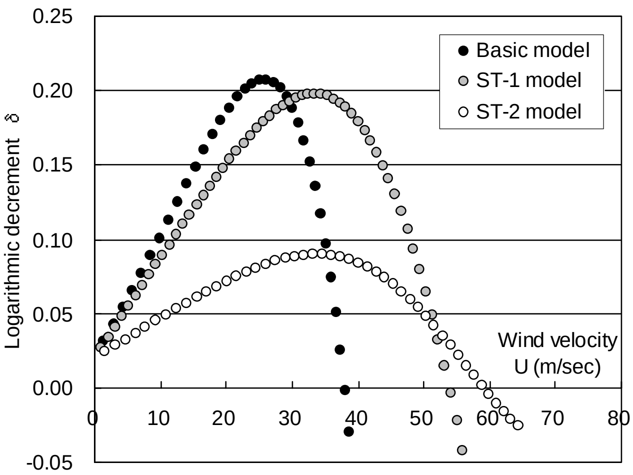

Fig.16 U-δ curve

6. Conclusions

As a result of this study, we found the following concerning the feasibility of all-plastic suspension bridges of the 5,000m-span class.

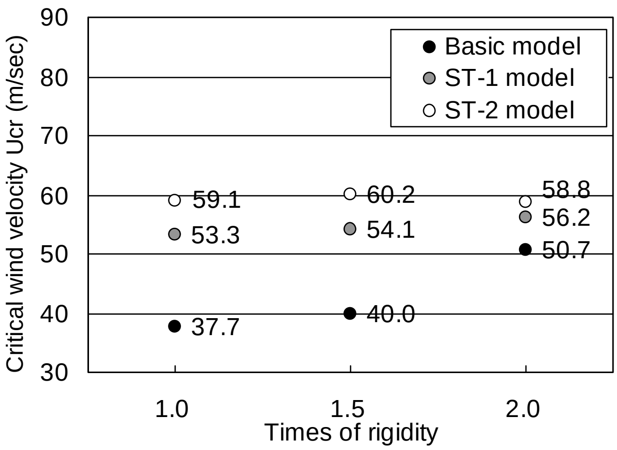

Fig.17 Effect due to Change of Torsional Rigidity

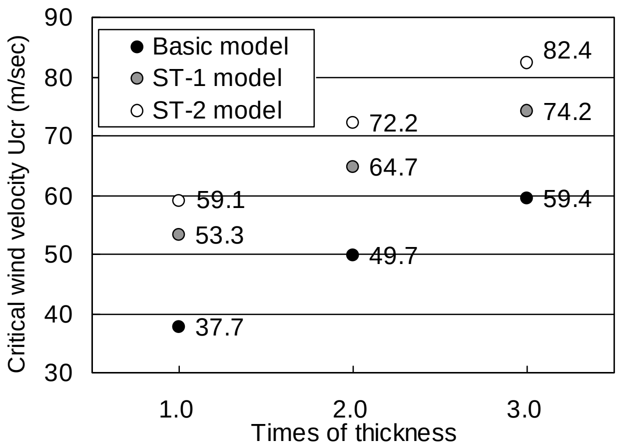

Fig.18 Effect due to Change of Plate Thickness of Stiffening Girder

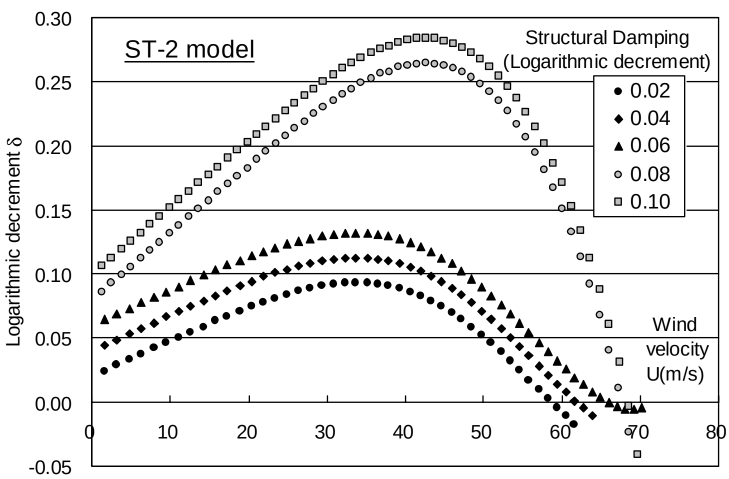

Fig.19 Effect due to Change of Structural Damping

(1) By using CFRP for the stiffening girder as well as for the main cable, a feasible design becomes possible even with the sag ratio of 1/20. As a result, the tower height can be restrained to about 300m, and the tower can be designed as CFRP and concrete composite columns. With the currently predominant ratio of 1/10, the tower height far exceeds 500m, making the feasibility low.

(2) The cross section of the stiffening girder is determined based on the stress due to the bending moment under design wind loads, and excess of allowable stress can be easily coped by making the stiffening girder locally nonuniform when the safety factor of material is required to be higher. There is no problem from the viewpoint of construction, including the structures of bands and saddles in which each strand is stored separately, because the sectional area of the main cable is sufficiently smaller than $1.0m^2$.

(3) Although the primary feature of the static structural characteristics is that displacements due to deflection are large both in-plane and out of plane, they are not the quantities which become the problems due to the vehicle travel and structural reliability. Even if the stiffening girder is designed to be continuous, only the negative bending moment at the intermediate support rapidly increases, and the effect in which their displacements are reduced is negligible.

(4) The aerodynamic stability against coupled flutter decreases markedly, but by adopting structural countermeasures (for example, the cross hanger, the horizontal cross-stay, etc.), the critical wind velocity can be ensured to the value of about 60m/sec. However, increasing the torsional rigidity of the stiffening girder merely by varying the shape of the cross section or the elastic shear coefficient of material does not appreciably improve the aerodynamic stability.

(5) In order to ensure the critical wind velocity to the value of about 70m/sec or 80m/sec, it may be necessary to make the plate thickness of the stiffening girder about 2 or 3 times the value decided from the static design, respectively. In contrast, when structural damping is sufficiently increased by installing an adequate damper system, the critical wind velocity can be ensured to about 70m/sec without greatly reducing the economical efficiency.

Therefore, although problems concerning, for example, the structure of hinge parts and the connection of pulltruded profiles, remain for future studies, the present results indicate that the feasibility of constructing all-plastic suspension bridges is not low.

References

[1] IABSE Publications Committee (WG23 New Materials), “Advanced Materials”, *Structural Engineering International*, Journal of IABSE, Vol.9, No.4, 1999.

[2] K. Maeda, Y. Morizono, H. Nakamura, T. Eguchi and Y. Fujino, “Applicability of CFRP Cables to Ultra Long-Span Suspension Bridges”, *Proc. of IABSE Conference in Seoul on Cable-Supported Bridges – Challenging Technical Limits*, CD-ROM (IABSE Report, Vol.84), 2001.

[3] T. Kawada, et al., “The modern suspension bridge”, *Rikohtosho*, 1987. (in Japanese and in Korean)

[4] N. Narita, K. Maeda, H. Nakamura, and K. Nomura, “Applicability of Dischinger-Type to Ultra-Long Span Bridges”, *Proc. of IABSE Symposium in Kobe on Long-Span and High-Rise Structures*, IABSE Report, Vol.79, pp.137-142, 1998.

[5] K. H. Ostenfeld (COWI Consult), “Bridges of Today and Tomorrow”, *10th Annual International Bridge Conference*, Pittsburgh, Pennsylvania, June 1993.

[6] M. Iwamoto, “Prediction of Aerodynamic Behavior of Cable Supported Bridges”, Ph. D. thesis, University of Tokyo, 1995. (in Japanese)